



Research article

Comprehensive analysis of prognosis of patients with GBM based on 4 m6A-related lncRNAs and immune cell infiltration

Qisheng Luo ^{a,1}, Zhenxiu Yang ^{b,1}, Renzhi Deng ^{c,1}, Xianhui Pang ^c, Xu Han ^c, Xinfu Liu ^c, Jiahai Du ^c, Yingzhao Tian ^c, Jingzhan Wu ^{c,**}, Chunhai Tang ^{c,*}

^a Department of Neurosurgery, Affiliated Hospital of Youjiang Medical University for Nationalities, BaiSe, Guangxi province, 533000, China

^b Department of Oncology, The Second Affiliated Hospital of Guangxi Medical University, NanNing, Guangxi province, 530000, China

^c Department of Neurosurgery (Trauma Surgery), The Second Affiliated Hospital of Guangxi Medical University, NanNing, Guangxi province, 530000, China



ARTICLE INFO

Keywords:

Glioblastoma multiforme
m6a methylation modification
lncRNA
Prognosis
Immune cell infiltration

ABSTRACT

Objective: To investigate the immune cell infiltration status in glioblastoma multiforme (GBM) and construct a novel prognostic risk model that can predict patients' prognosis.

Methods: The Cancer Genome Atlas (TCGA) database was used to obtain RNA-sequence information and relevant clinical data. We performed Pearson correlation, univariate Cox regression to screen m6A-related prognostic lncRNA. GBM patients' samples were separated into different clusters through the ConsensusClusterPlus package. The risk score model was established through LASSO regression analysis. Besides, KEGG pathway enrichment analysis was implemented. CIBERSORT algorithm was used to analyze the difference of 22 types of immune cell infiltration in different cluster of GBM patient. Cox regression analyses were used to verify the independence of the model and correlation analysis was performed to demonstrate the link between our model and clinical characteristics of GBM patients. Experiments were used to validate the differential expression of the model lncRNA in patients with different prognosis.

Results: 17 lncRNA related to prognosis were screened from 1021 m6A-related lncRNAs. Further, four m6A-related lncRNAs that were significantly correlated with GBM prognosis were selected to establish our prognostic risk model, which had excellent accuracy and can independently predict the prognosis of GBM patients. The infiltration fractions of T regulatory cells, T cells CD4 memory activated and neutrophils were positively associated with risk score, which suggested a significant relationship between the model and tumor immune microenvironment.

Conclusion: The m6A-related RNA risk model offered potential for identifying biomarkers of therapy and predicting prognosis of GBM patients.

1. Introduction

Glioblastoma multiforme (GBM), a type of intracranial tumor originating from normal brain cells or lower-grade astrocytoma, was the one of the most aggressive malignant CNS cancers taking up 47.7% of all cases [1]. This cancer often happened in the elderly, with

* Corresponding author.

** Corresponding author.

E-mail addresses: tiger.2000@163.com (J. Wu), tangch7907@163.com (C. Tang).

¹ The first three author contributed equally to this work.

<https://doi.org/10.1016/j.heliyon.2023.e12838>

Received 14 February 2022; Received in revised form 25 December 2022; Accepted 3 January 2023

Available online 5 January 2023

2405-8440/© 2023 Published by Elsevier Ltd.

This is an open access article under the CC BY-NC-ND license

(<http://creativecommons.org/licenses/by-nc-nd/4.0/>).

the five-year relative survival rate being only 6% [2]. Despite intensive research in its treatments including surgical resection, chemotherapy and radiotherapy, its prognosis remained poor and the average survival time was merely 12–18 months [3]. Therefore, it was still urgent to search for new prognostic-related therapeutic targets of the therapy and prognosis of glioblastoma.

Occurring in the N6-position of adenosine, N6-methyladenosine (m6A) was the most prevalent epigenetic modification on mRNA of major eukaryotic species [4,5]. It involved in RNA splicing, mRNA decay and the production of long-non-coding RNA (lncRNA), ect [6]. Accumulating evidence revealed that m6A RNA modification was achieved by the interaction between “writers” (methyltransferases), “readers” (binding proteins) and “erasers” (demethylase) [5]. These were the proteins that can add, identify and clear m6A-modified sites, thus changing various biological processes [7]. Due to its role in regulating apoptosis, cell differentiation and self-renewal of stem cells through modulating gene expression, N6-methyladenosine (m6A) RNA methylation was considered to be associated with tumor progression [8]. A recent study showed that there was a significant acceleration in HCC cell (Hepatocellular carcinoma) proliferation and migration in condition of METTL3 overexpression as this up-regulation increased m6A methylation of the tumor suppressor SOCS2, eventually inducing its degradation [9]. As two essential m6A regulators, inhibition of miR-493-3p and overexpression of YTHDF2 contributed to a decreased m6A level, involving in prostate cancer progression [10]. Qi Cui et al. revealed that knockdown of METTL3 or METTL14, which were two components of RNA methyltransferase complex of m6A modification, can induce GSC (glioblastoma stem cell) growth and oncogenesis [11].

Aberrant expression of lncRNA also linked to tumor progression, which influenced chromatin organization, transcription and post-transcription, thus conferring the oncogenicity for cancer development [12]. A research in 2018 revealed that the up-regulation of lncRNA HOTAIRM1 promoted oncogenesis through regulating the expression of HOXA1 gene, which was an oncogene inducing cell proliferation and invasion in GBM [13]. Additionally, a high expression level of lncRNA SNHG15 was correlated with GBM tumorigenesis and the suppression of this lncRNA contributed to a decrease in tumor cell proliferation [14]. Although there were numerous studies about lncRNAs and glioblastoma, the connection between m6A-related lncRNAs and GBM remained elusive. Here we focused on investigating the relationship between m6A-related lncRNAs and glioblastoma multiforme.

In this research, we first extracted the expression profiles of lncRNAs and m6A genes from The Cancer Genome Atlas (TCGA) dataset. Next, by using Pearson correlation analysis, we determined the m6A-related lncRNAs, based on which we classified patients with GBM into two clusters. In addition, the clinical outcomes of the two types of patients were significantly distinctive, indicating that these lncRNA were related to the prognosis. Therefore, they were further screened and used to construct our prognostic evaluation model for predicting overall survival time of patients. Through the verification of external data sets, it was proved that this model had excellent efficiency and can accurately predict the prognosis of patients with GBM. Furthermore, we investigated immune microenvironment by analyzing the infiltration fraction of various immune cells.

2. Materials and methods

2.1. Collection and processing of data

Inclusion criteria of patient: Gliomas of World Health Organization (WHO) grade IV was defined as Glioblastoma multiforme (GBM). The patient had complete basic clinical data and survival data. Exclusion criteria: GBM patients with missing OS values or OS < 30 days were excluded in order to reduce statistical bias in our analysis. Patients who had received radiotherapy or chemotherapy before surgery (before sequencing tumor samples).

We downloaded the mRNA expression files [Fragments Per Kilobase of transcript per Million mapped reads (FPKM) normalized] of GBM in TCGA from the Xena website (<https://xena.ucsc.edu/>). The RNA sequences and relevant clinical information of 169 tumor samples from GBM patients were extracted from the TCGA database. The mRNA-seq data and related informations of GBM patients was downloaded from the CGGA database (<http://www.cgga.org.cn/>). The corresponding information of 1157 normal samples were downloaded from GTEx database, with all the RNA sequences being normalized. These genes were split into two groups according to the data of human genome annotation. They were lncRNA genes group and protein-coding genes group respectively and we extracted 23 m6A regulatory genes from the latter group. In order to assess the correlation between the 23 m6A regulatory genes and lncRNAs, Pearson correlation coefficient analysis was conducted and we defined m6A-related lncRNAs as lncRNAs with P value < 0.05 and absolute correlation coefficient > 0.4.

2.2. Evaluation of m6A-related lncRNA survival

We associated RNA sequence data of GBM patients with their clinical data. Also, we performed Univariate Cox regression to analyze the connection between the survival time of GBM patients and the expression level of m6A-related lncRNAs, with P < 0.05 being statistically significant. Eventually, 17 m6A-related prognostic lncRNAs were screened.

2.3. Clustering and annotations of 17 m6A-related lncRNAs

The expression data of m6A related prognostic lncRNA in 169 GBM patients were extracted and subsequently a consensus clustering of patients was performed according to the expression of lncRNA using the tool “ConsensusClusterPlus”, which aimed to understand the biological implications of the 17 m6A-related prognostic lncRNAs. (sampling rate 80%, 50 iterations) We also created heatmap using pheatmap package, which helped to detect the differences of various m6A-related prognostic lncRNAs expression level between two clusters, and explored the connection between lncRNAs and corresponding clinicopathological characteristics. Limma

package was used for detecting the distinctive expression of target genes in different clusters and analyzing gene correlation with $P < 0.05$ being statistically significant. We obtained the standard names of the target genes from NCBI (<https://www.ncbi.nlm.nih.gov/>). Next, Kyoto Encyclopedia of Genes and Genomes (KEGG) pathway enrichment analysis was implemented, which was also combined with cluster analysis packages to functionally determine the distinction of molecular pathways among various m6A-related lncRNA expression modes. Additionally, we performed Gene set enrichment analysis (GSEA) to detect the features of tumors in GBM subgroups.

2.4. Analysis of immune cell infiltration in tumor microenvironment of GBM

The penetration of TME in two clustering patterns were analyzed. According to standardized gene expression profiles, CIBERSORT algorithm was used to evaluate 22 different immune cell types in tumor samples by featuring the cellular components of tissues. Limma package was used for analyzing the distinctive infiltration fraction of immune cells in the two clusters. The differences of infiltration fraction were depicted using vioplot and the infiltration fractions of various kinds of immune cells were presented in boxplot. Finally, limma package was used to study the differences of TME in the two clusters based on stroma score, immune score and ESTIMATE score, which we presented on boxplots.

2.5. Screening of prognostic value and risk signal establishment of m6A-related lncRNA

To find the prognostic features of m6A-related lncRNAs of the training set, Univariate Cox regression analysis and least Absolute Shrinkage and Selection Operator (LASSO) were implemented. Also, we used the least absolute shrinkage and selection operator (LASSO) regression algorithm to screen the characteristics, plus 10-fold cross-validation. These analyses used the R software package glmnet (v 4.1–1). We used the following formula to calculate the risk scores for GBM patients: Risk score = $SE_{\text{Exp1}} \times \text{IncRNA1} + SE_{\text{Exp2}} \times \text{IncRNA2} + SE_{\text{Exp3}} \times \text{IncRNA3} + \dots + SE_{\text{Expn}} \times \text{IncRNAn}$. $SE_{\text{Exp}i}$ indicated the coefficient of each lncRNA and lncRNAn represented the expression of each lncRNA. We also performed receiver operating characteristic (ROC) curve analysis to estimate the efficacy of lncRNA signatures in the test and training set. Univariate Cox proportional hazards regression was used to create P value and hazard ratio (HR) with 95% confidence interval (CI). Additionally, we performed R packages and all methods above using R software version 4.0.3 (The R Foundation for Statistical Computing, 2020), with $P < 0.05$ defined as statistically significant.

2.6. Establishment of risk signal and verification

The TCGA group was randomly split into two subgroups: a training set and a test set. The training set was used to build the m6A-related lncRNA model while the test one was for validating the model. No significant difference of clinical characteristics was detected between the two sets ($P > 0.05$). Combined with the GBM survival information of TCGA, we selected 17 m6A-related prognostic lncRNAs from 1035 m6A-related lncRNAs in TCGA data by univariate cox regression analysis. Further LASSO Cox regression analysis (using penalty parameters estimated by 10-fold cross validation) performed by R-package glmnet found that 4 m6A-related lncRNAs were significantly connected with the OS of GBM patients from TCGA dataset. Then, we used multivariate Cox regression and LASSO analysis to establish a risk model of four m6A-related lncRNAs. The following formula was used for calculating the risk score: Risk score = $\text{Coef}(\text{IncRNA1}) \times \text{expr}(\text{IncRNA1}) + \text{coef}(\text{IncRNA2}) \times \text{expr}(\text{IncRNA2}) + \dots + \text{coef}(\text{IncRNAn}) \times \text{EXPr}(\text{IncRNAn})$. In this formula, coef represented coefficient, expr (lncRNAn) indicated the expression of lncRNAs and coef (lncRNAn) was the coefficient of lncRNAs related to survival. Taking the median risk score as the dividing line, patient samples in the training set were divided into high-risk group and low-risk group.

2.7. Independence and correlation analysis of m6A-related lncRNA risk model

We used multivariate and univariate Cox regression analyses to study the independence of our four m6A-related lncRNA risk model. Therefore, we can determine whether this model was an independent variable when other clinical features of patients with GBM such as gender and age varied. Also, heatmap was produced using the limma package and the pheatmap package. Besides, according to the clinical information, we created boxplots of relationship between risk scores and clinical features. In addition, we used correlation analysis to prove the link between the risk model and clinical features of GBM. We also performed genetic difference analysis to assess distinctive expression of target genes in the low-risk and high-risk groups. Scatterplots were used to describe the connection between m6A-related lncRNA risk model and immune-infiltrating cells.

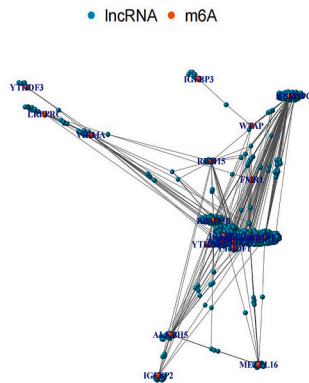
2.8. Experimental validation results of m6A-related prognostic lncRNA

From September 2018 to September 2020, 40 patients with stage II and IV GBM in the First Affiliated Hospital of Guangxi Medical University were screened, with 20 patients in each stage. Inclusion criteria: (1) Pathologically confirmed cases (2) New cases first diagnosed in this hospital. Exclusion criteria: (1) The patient had or not other malignant tumors. (2) Patients receiving preoperative radiotherapy, chemotherapy or other antitumor drugs. Tumor tissue and normal tissue samples were collected from the surgical patients (tissues further than 5 cm from the periphery of tumor tissue were regarded as normal tissues). Using GAPDH as internal reference, qPCR was conducted to detect the expression of selected RNA. Primers were listed in Table 1. With the expression level of GAPDH as the standard value 1, the relative expression levels of 4 types of RNA in the tumor tissues of stage I and III patients were

Table 1
qPCR primers for genes related to prognosis.

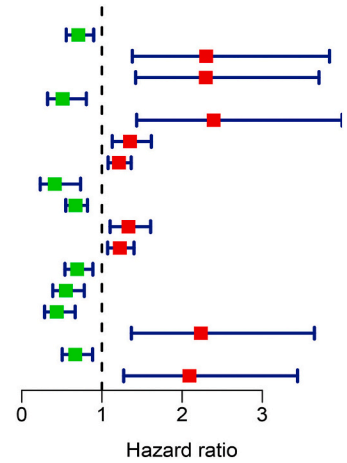
Gene	DLEU1	AC005005.3	ZEB1-AS1	UNC5B-AS1	GAPDH
Forward Primer	TGCATTTAAAACCGCCCTGC	GGGATCGTGTCCACAAGTTCA	GAACCGGGATGGGAAGTGAC	GATCCTGCCTCAGGGAAA	ACAAC TTTGGTATCGTGGAAGG
Reverse Primer	TTGAAGAAGGAGACACGCC	GCTACTCCTCGTTGCTCCTT	GGTTCTACGCGAGGAAGAGG	GCTCAAGAGGTTGGGACT	GCCATCACGCCACAGTTTC

A

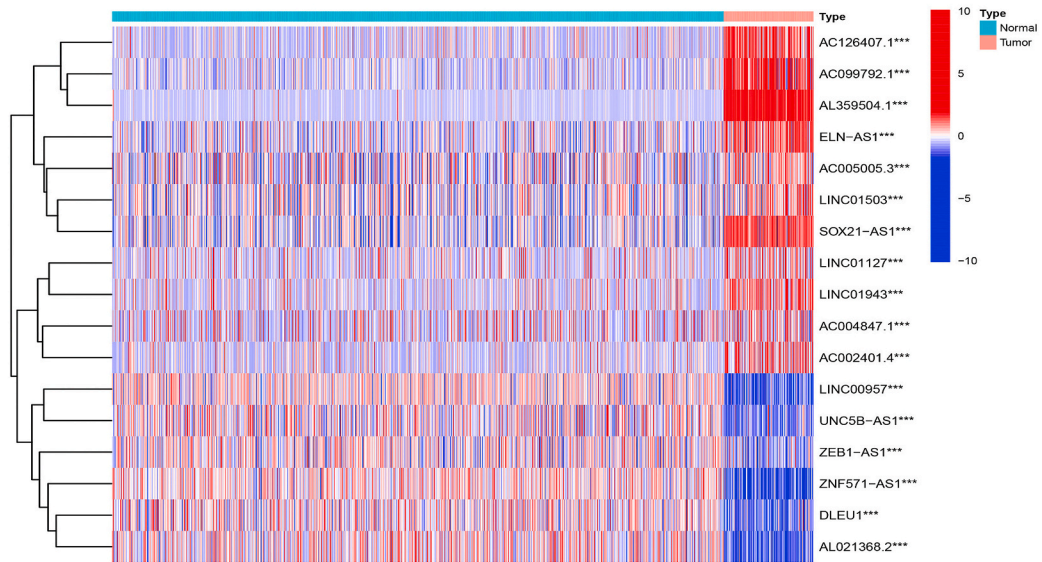


B

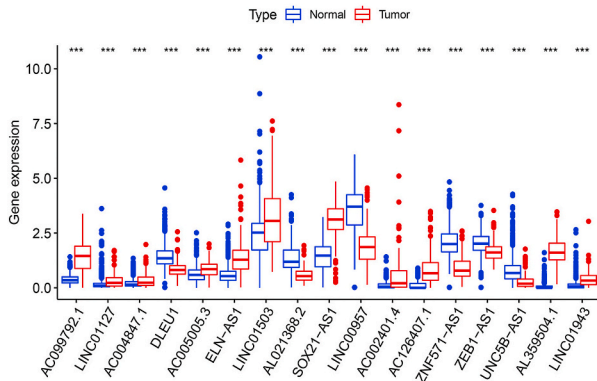
	pvalue	Hazard ratio
AC099792.1	0.004	0.706(0.555-0.897)
LINC01127	0.001	2.300(1.379-3.838)
AC004847.1	<0.001	2.295(1.421-3.707)
DLEU1	0.004	0.509(0.322-0.806)
AC005005.3	<0.001	2.393(1.433-3.994)
ELN-AS1	0.001	1.350(1.128-1.616)
LINC01503	0.001	1.212(1.077-1.365)
AL021368.2	0.003	0.412(0.231-0.734)
SOX21-AS1	<0.001	0.671(0.549-0.820)
LINC00957	0.003	1.331(1.102-1.607)
AC002401.4	0.003	1.224(1.071-1.400)
AC126407.1	0.004	0.691(0.538-0.887)
ZNF571-AS1	<0.001	0.550(0.387-0.780)
ZEB1-AS1	<0.001	0.436(0.285-0.666)
UNC5B-AS1	0.001	2.234(1.367-3.650)
AL359504.1	0.005	0.667(0.504-0.884)
LINC01943	0.004	2.091(1.271-3.439)



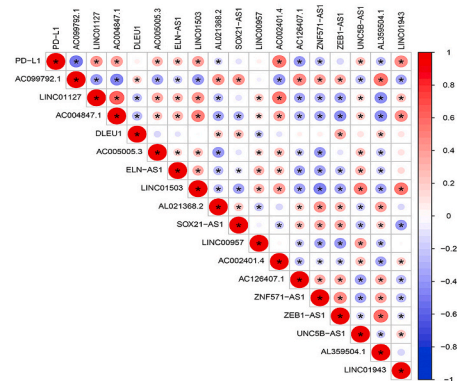
C



D



E



(caption on next page)

Fig. 1. Identification and expression of m6A-related lncRNAs in GBM (A): Network diagram of correlation between m6A regulating genes and lncRNAs. (B): Forest plot of univariate Cox regression analysis of relationship between the survival time of GBM patients and the expression of m6A-related lncRNA. Green represents low risk. (C): Heatmap of the differences in the expression of m6A-related prognostic lncRNAs between tumor and normal tissues. * $P < 0.05$. Red represents high expression, while blue represents low expression. (D): Boxplot of different expression of m6A-related prognostic lncRNAs in both tumor and normal tissues. * $P < 0.05$. (E) Correlation analysis to show the correlation between target gene *PD-L1* and m6A-related prognostic lncRNAs in GBM. Red presents the positive correlation, while blue presents the negative correlation. * means a statistically significant difference. (For interpretation of the references to color in this figure legend, the reader is referred to the Web version of this article.)

calculated, and the statistical graph was drawn.

2.9. Statistical analysis

We used R software (version number v3.5.2) to analyze statistics and performed Kaplan-Meier method to determine the overall survival rates. Then, log-rank was used for analyzing the significant difference of survival rates in various groups. In addition, Wilcoxon signed rank-sum test was used for comparing the infiltration fraction of immune cells in different groups. In all the correlation analyses, $P < 0.05$ was considered as the significance threshold.

3. Results

3.1. Expression of M6A methylation regulation factor in glioma and identification of related lncRNAs

M6A RNA methylation regulation factor played a significant role in the progression of cancers. Therefore, we studied the expression profiles of 23 m6A methylation regulation factor in GBM. To identify potential M6A-related lncRNAs, Pearson correlation coefficient was performed to analyze the connection between M6A methylation regulators and lncRNAs. Results showed that we identified 1867 interactions and 1035 m6A-related lncRNAs (absolute correlation coefficient >0.4 , $P < 0.05$). The relationship between M6A methylation regulation factor and related lncRNAs was shown in Fig. 1A.

3.2. Expression of M6A-related prognostic lncRNA in glioma

We used univariate Cox regression analysis to screen prognosis-related M6A-related lncRNAs from 1035 M6A-related lncRNAs in TCGA RNA-seq data sets. The seventeen M6A-related lncRNAs in the TCGA dataset were correlated with OS (Fig. 1B). Fig. 1C showed the thermographic analysis, which was used to compare the expression of M6A-related lncRNA in tumor and normal tissues. Compared with normal tissues, the expression levels of AC099792.1, LINC01127, AC004847.1, AC005005.3, ELN-AS1, LINC01503, SOX21-AS1, AC002401.4, AC126407.1 and AL359504.1 were significantly higher in tumor tissues. On the contrary, tumor tissues had lower expression level of DLEU1, AL021368.2, LINC00957, ZNF571-AS1, ZEB1-AS1, UNC5B-AS1 and LINC01943 compared to normal tissues (Fig. 1D). Correlation between m6A-related prognostic lncRNA in the whole genome of TCGA was presented in Fig. 1E.

3.3. Consensus cluster analysis of m6A-related prognostic lncRNAs to distinguish different subgroups with different prognosis

Consensus cluster analysis indicated that in the range of $k = 2-9$, the clustering result was the most stable when $k = 2$. The results of consensus clustering indicated that GBM patients could be split into two clusters with high stability (Fig. 2A-L). The expression levels of m6A-related lncRNA in cluster 1 and cluster 2 were analyzed and there was a significantly higher expression of lncRNA (UNC5B-AS1, ELN-AS1, LINC00957, LINC01503, LINC01943, AC005005.3, AC002401.4, LINC01127, AC004847.1) in cluster 2 than cluster 1. In contrast, the expression level of lncRNA (DLEU1, SOX21-AS1, AL021368.2, ZNF571-AS1, ZEB1-AS1, AL359504.1, AC099792.1, AC126407.1) was much upregulated in cluster 1 than that in cluster 2 (Fig. 3A). Previous research revealed that CD274 was associated with GBM. For instance, in the presence of temozolomide (TMZ) which was a drug for GBM therapy, GBM cells inhibited the expression of pro-inflammatory cytokines in activated periphery blood mononuclear cells, which relied on upregulated expression of CD274 [15]. Therefore, we further investigated the expression level of CD274 in different subgroups. The expression level of CD274 was higher in tumor tissues than normal tissue and was also higher in patients in cluster 2 than that in cluster 1 (Fig. 3B, C). Furthermore, we studied the clinicopathological characteristics of these two clusters of patients. The OS of patients in cluster 2 was worse than that of patients in cluster 1. ($p < 0.001$) Additionally, the difference in the one-year OS of patients in cluster 1 was nearly three times larger than that in cluster 2 (Fig. 3D). The above results indicated that clusters determined by expression of m6A-related prognostic lncRNAs were related to CD 274 and patients' prognosis.

3.4. The influence of m6A-related prognostic lncRNA expression on signaling pathways and biological processes

GSEA was implemented to explore different mechanisms between the two clusters, which helped us to identify the roles of various m6A-related lncRNAs in GBM progression. According to the results of Kyoto Encyclopedia of Genes and Genomes (KEGG) enrichment analysis, JAK-STAT signaling pathway, cytokine-cytokine receptor interaction, natural killer cell mediated cytotoxicity, cell adhesion molecules and chemokine signaling pathway were significantly enriched in cluster 2, which may be dramatically associated with tumor metastasis and progression. Purine metabolism, spliceosome, cell cycle and wnt signaling pathway were enriched in cluster 1

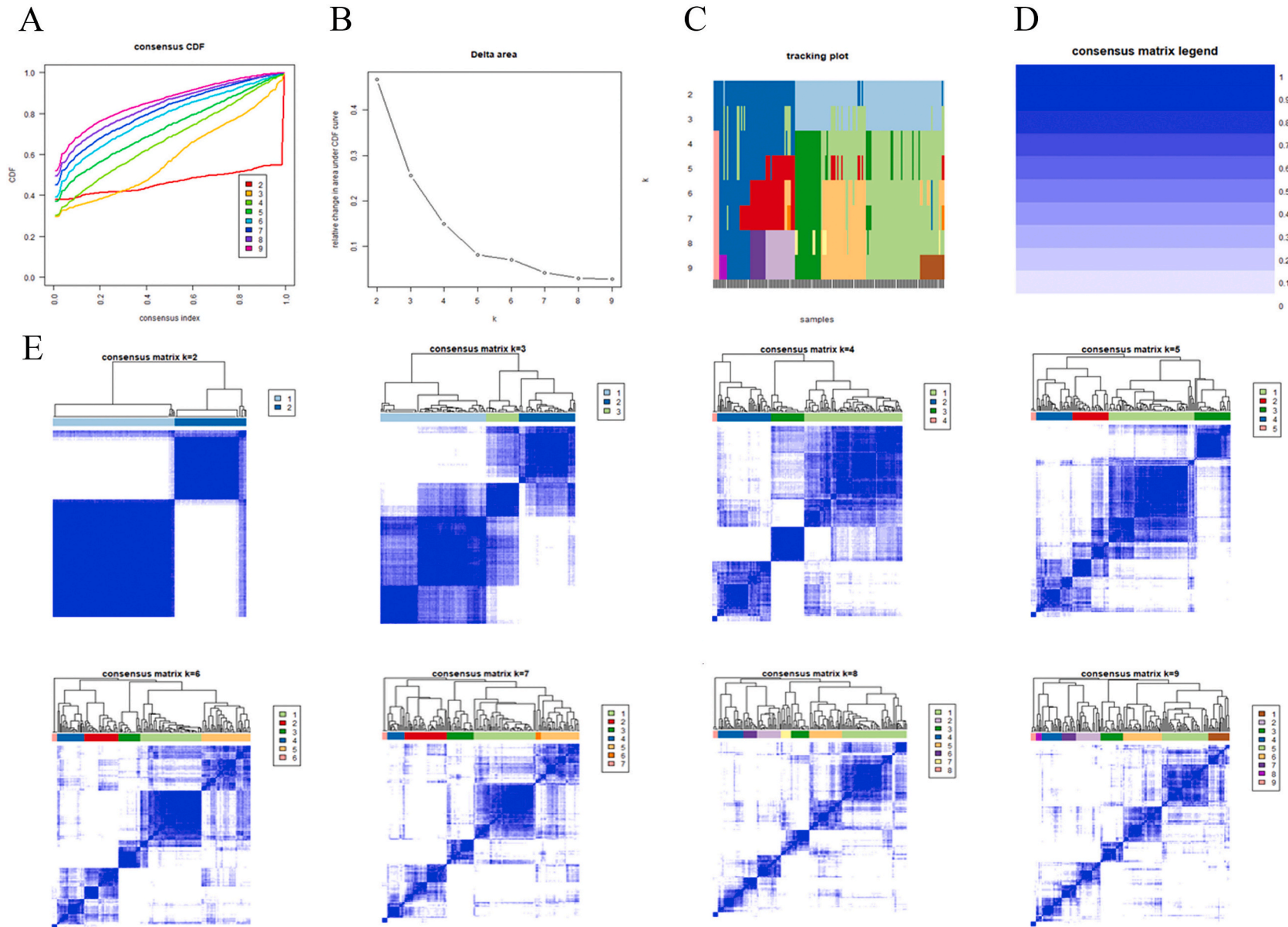


Fig. 2. Consensus cluster analysis of m6A-related prognostic lncRNAs (A–D): The results of consensus clustering by using ‘ConsensusClusterPlus’. When $k = 2$, the clustering results were the most stable. E: visualization of clustering results when patients are sequentially classified into 2–9 clusters.

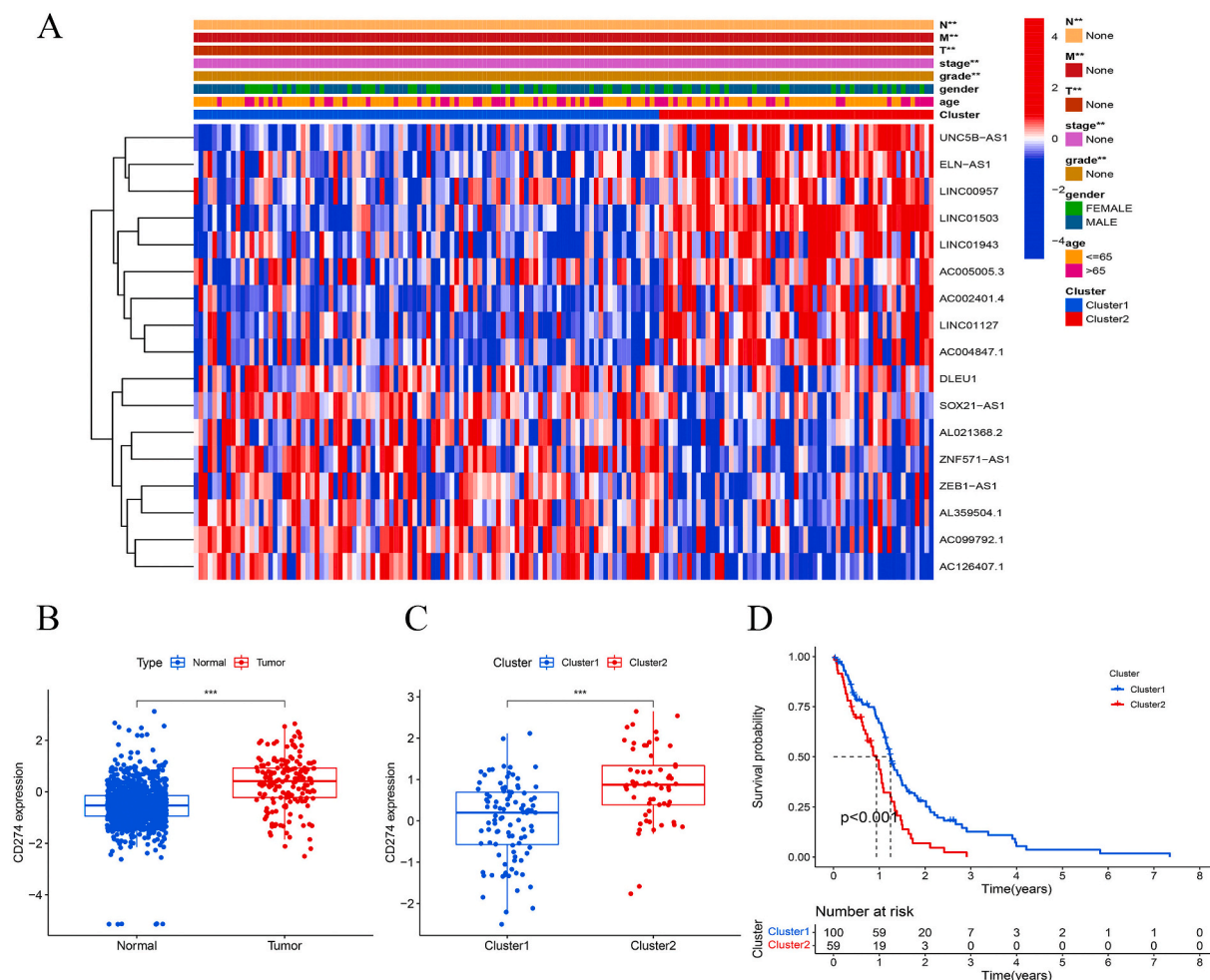


Fig. 3. The expression and relationship of m6A-related prognostic lncRNA and PD-L1 in different clusters. (A): Heatmap of differences in the expression of m6A-related prognostic lncRNAs associated with clinicopathological parameters in different clusters. * $P < 0.05$. (B): Differences in the expression of PD-L1 in different clusters. * $P < 0.05$. (C): Differences in the expression of PD-L1 in normal and tumor tissue. (D): Survival analysis of cluster 1 and cluster 2. $P < 0.001$.

(Fig. 4). The above results indicated that there was a close relationship between m6A-related prognostic lncRNAs and GBM prognosis, which may involve multiple signaling pathways.

3.5. Characteristics of cell infiltration in tumor microenvironment with different M6A modification modes

As this study suggested that the expression of GBM m6A-related prognostic lncRNA was closely related to immune response, we next analyzed the infiltration features of cells under different M6A-related lncRNA modes in tumor microenvironment (TME).

We analyzed the penetration of TME in the two clusters, and finally used CIBERSORT algorithm to evaluate 22 different immune cell types in 169 samples. We calculated the median absolute score of 22 cell types in each cluster given by CIBERSORT (Fig. 5A). The results revealed that the infiltration fraction of T cells regulatory (Tregs) in cluster 2 was significantly higher than that in cluster 1 (Fig. 5B). Similarly, the number of T cells CD8 and T cells CD4 memory activated in cluster 2 was significantly higher than that in cluster 1 (Fig. 5C, D). In contrast, the fraction of mast cells activated was higher in cluster 1 than that in cluster 2 (Fig. 5E). Next, we used the ESTIMATE algorithm to score immune cell infiltration in cluster 1 and cluster 2. The results revealed that cluster 2 showed higher ESTIMATE score ($P < 0.0001$), immune score ($P < 0.0001$) and stroma score ($P < 0.0001$) (Fig. 5F–H). The TME of cluster 2 significantly increased the infiltration of immune cells, which confirmed these findings.

3.6. Construction and verification of m6A-related lncRNAs risk model in GBM patients

A total of 159 patient samples were randomly divided into a training data set ($N = 80$) and a test data set ($N = 79$). We selected 17 M6A-related prognostic lncRNAs from 1035 M6A-related lncRNAs in TCGA data set by cox regression analysis based on GBM survival

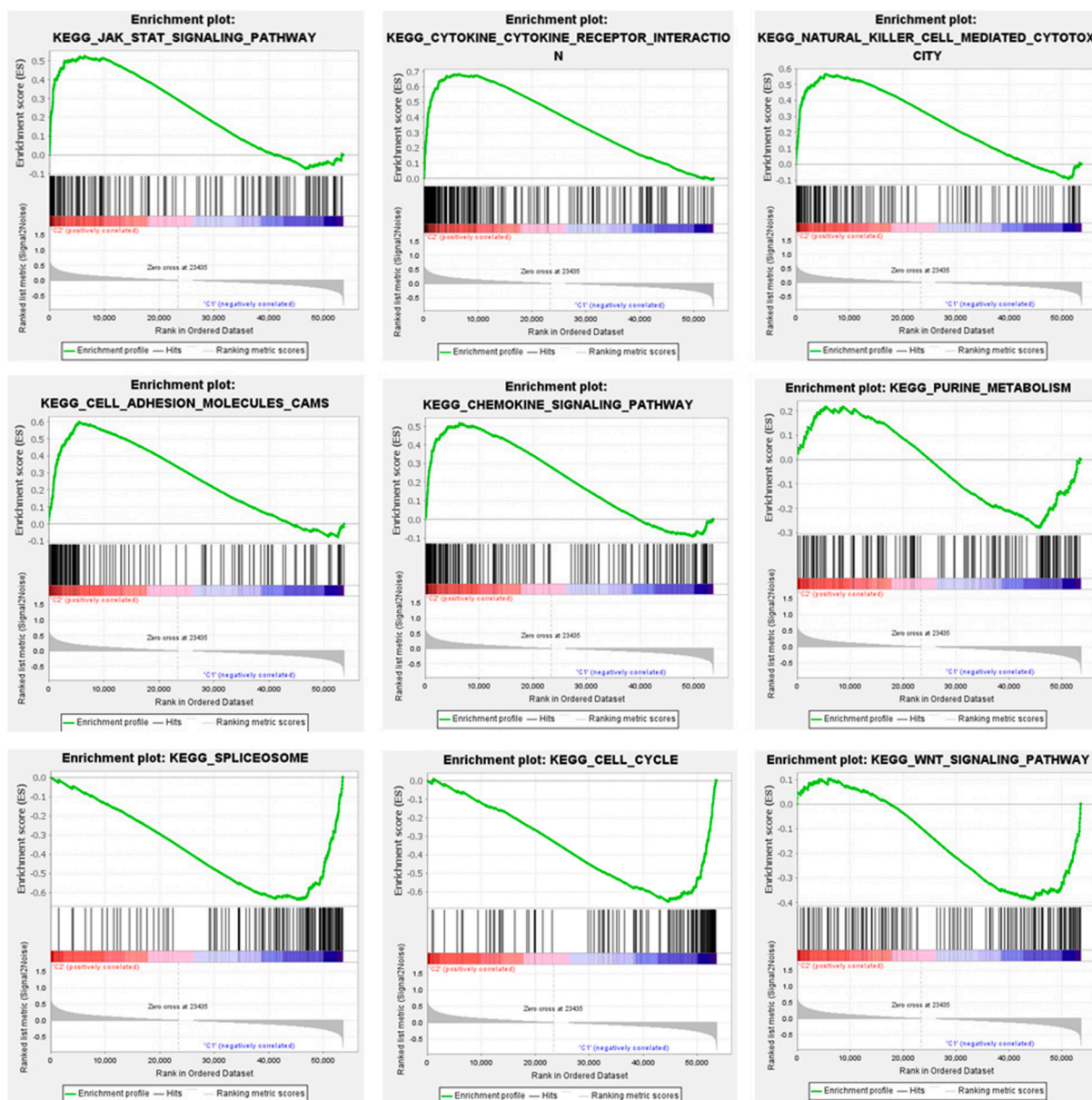
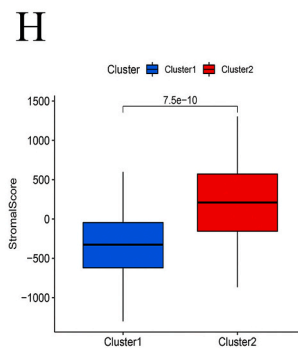
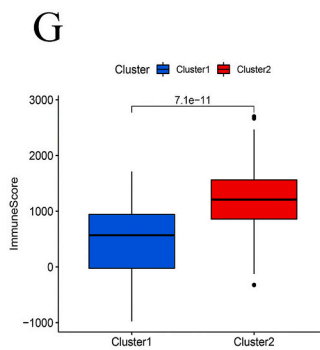
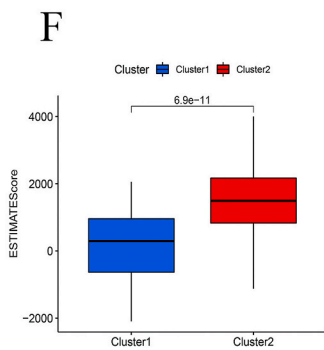
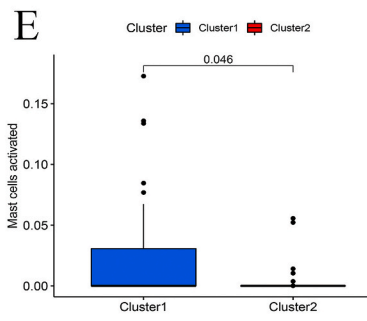
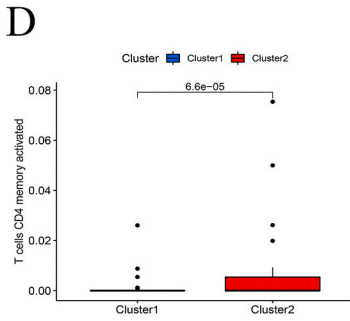
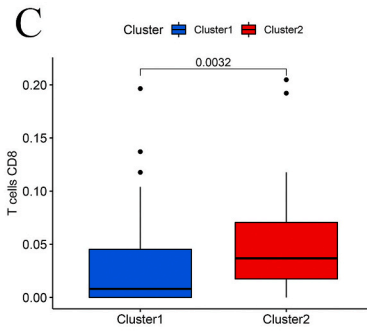
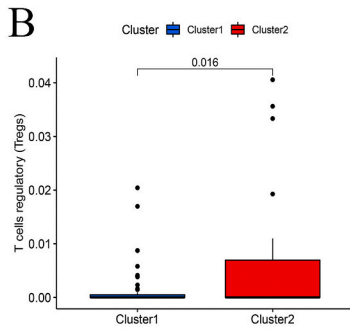
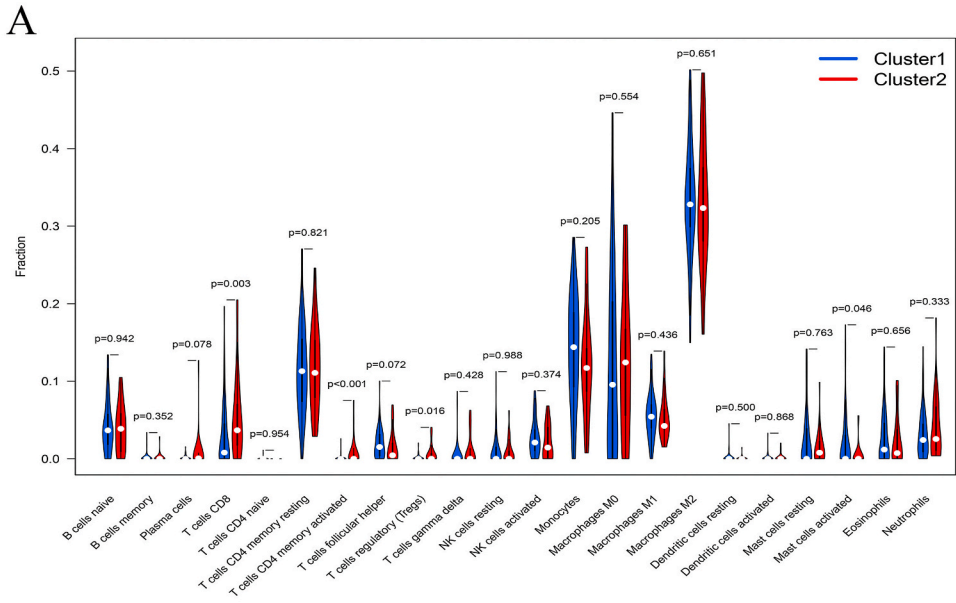


Fig. 4. KEGG enrichment analysis

The top 9 enriched signaling pathways were listed. Both FDR q -value and FWER p -value were < 0.05 .

data of TCGA (Table 2). But further LASSO regression analysis found that 4 M6A-related lncRNAs were more closely correlated with the OS of GBM patients and finally a four-m6A-related lncRNA risk model was established (Fig. 6A and B). In the training set, samples of patients were further separated into high-risk group and low-risk group according to the median risk score. Fig. 6C indicated the risk score distribution between high-risk group and low-risk group. Moreover, the survival time and survival status of patients in the two risk groups were presented in Fig. 6D. The relative expression levels of four M6A-related lncRNAs for each patient were shown in Fig. 6E. Survival analysis showed that the OS of the low risk group was longer than that of the high risk group ($p < 0.001$) (Fig. 6F). Besides, in the training set, the area under the curve (AUC) of the 5-year overall survival rate was 0.795, which meant that the lncRNA feature had a good accuracy in the prediction of GBM patients' prognosis (Fig. 6G).

For testing the prognostic evaluation ability of our new model, we used a unified formula to calculate the risk score of each patient in the test group. The distribution of risk levels, the mode of survival status and survival time, and the M6A-related lncRNAs expression in the test set were shown in Fig. 7A–C, respectively. The Kaplan-Meier survival analysis showed that the OS of the low-risk group was longer than that of the high risk group ($p < 0.05$) (Fig. 7D). Additionally, Fig. 7E indicated that the area under the curve (AUC) of the 5-year overall survival rate was 0.773. This demonstrated that there was no significant difference in prognosis outcomes between the



(caption on next page)

Fig. 5. Cell infiltration characteristics of tumor microenvironment. (A): Vioplot of differences in infiltration of 22 types of immune cells in different clusters. (B–H): Boxplot of the analysis of differences in immune cell infiltration in different clusters. $P < 0.05$. (I–K): Boxplot of the analysis of differences in tumor immune microenvironment in different clusters.

Table 2

The 17 m6A-related prognostic lncRNAs in GBM.

Gene	HR	HR.95L	HR.95H	pvalue
AC099792.1	0.705912129	0.555273182	0.897417613	0.004458659
LINC01127	2.300184241	1.378707429	3.837541913	0.001424168
AC004847.1	2.295069546	1.420793079	3.707326775	0.000685238
DLEU1	0.509206254	0.321779735	0.805802794	0.003951965
AC005005.3	2.392600274	1.433337085	3.99385192	0.000846653
ELN-AS1	1.349773134	1.127601943	1.615718672	0.001080196
LINC01503	1.212359993	1.076850217	1.364922186	0.001451148
AL021368.2	0.411616871	0.230791268	0.734119838	0.002638425
SOX21-AS1	0.671041477	0.549125057	0.820025707	9.64E-05
LINC00957	1.330508201	1.101563321	1.607036146	0.003036928
AC002401.4	1.224380454	1.070714272	1.400100415	0.00309112
AC126407.1	0.690873245	0.538210985	0.886837791	0.003700945
ZNF571-AS1	0.549661641	0.387265637	0.780156799	0.000809768
ZEB1-AS1	0.435642885	0.285150122	0.66556073	0.000121648
UNC5B-AS1	2.233741904	1.36693546	3.650211029	0.001339366
AL359504.1	0.667396514	0.503702337	0.884288348	0.004855401
LINC01943	2.091048147	1.271261533	3.43948294	0.003669988

training group and the test group.

Based on the general clinicopathological features, the differences of operating systems were stratified and analyzed between the high-risk and low-risk groups. According to the subgroups classified by sex and age, the OS of the low-risk group was better than that of the high-risk group. It indicated that the m6A-related lncRNAs risk model can be applied to people with different clinical subgroups (Fig. 8 A-D).

3.7. The risk score evaluation of different groups

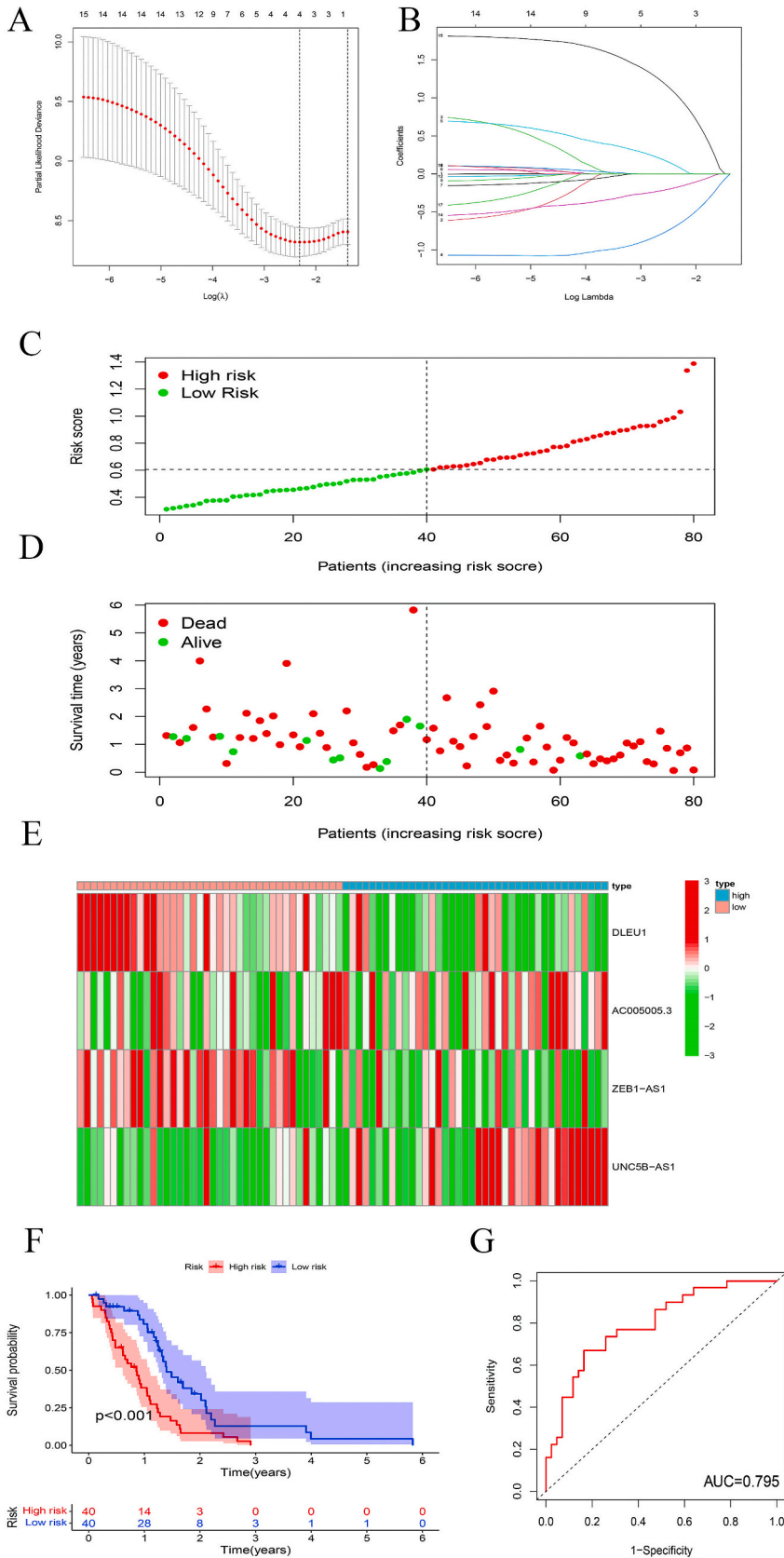
Fig. 8E indicated that the risk score was significantly higher in the group with high immune score than that in the group with low immune score ($p < 0.0001$). Besides, the risk score of cluster 1 was significantly lower than that of cluster 2 ($p < 0.0001$) (Fig. 8F). The screening of independent prognostic risk factors showed that the hazard ratio (HR) of risk score was 2.41 and 95% confidence interval (CI) was 1.49–3.88 ($p < 0.001$). The above results demonstrated that m6A-related lncRNAs were the independent prognostic factor of OS in GBM and they were not related to age, gender, grade and stage (Fig. 8G). The relative expression levels of four m6A-related lncRNAs in high-risk and low-risk groups were shown in Fig. 8H. We found that the expression levels of both DLEU1 and ZEB1-AS1 were higher in low-risk group than that in high-risk group. On the contrary, both AC005005.3 and UNC5B-AS1 were expressed more in high-risk group than that in low-risk group. Despite of this, as PD-L1 involved in cancer progression, we analyzed its expression but found no significant difference between low-risk and high-risk groups (Fig. 9A). Furthermore, we analyzed the differences in risk scores among various GBM subgroups to identify the clinical significance of the 4 lncRNAs in patients. We found that there was no significant difference in risk score between female group and male group, and between group aged over 65 and group aged less than or equal to 65 (Fig. 9B and C). The above results suggested that there was no connection between risk scores and age or gender while immune score, clusters were dramatically related to risk scores.

3.8. The relationships between various immune-infiltrating cells and risk scores

As our risk model indicated a connection with immune response pathways, we explored the relationship between immune-infiltration cells and m6A-related lncRNA risk model score. Fig. 9D showed that the infiltration fraction of T cells regulatory had a significantly positive correlation with the risk score ($p < 0.05$). Similarly, the infiltration fraction of both T cells CD4 memory activated and neutrophils had a significantly positive connection with the risk score, which were indicated in Fig. 9E and F respectively ($p < 0.05$).

3.9. qPCR validation results of prognostic related lncRNA

Baseline data of GBM patients had no significant difference. Fig. 9G showed the results of qPCR of prognostic related lncRNAs. The expression of lncRNA DLEU1 and ZEB1-AS1 in tumor tissues of stage III patients was lower than that in stage I patients. The expression of lncRNA AC005005.3 and UNC5B-AS1 in tumor tissues of stage III patients was higher than that in stage I patients.



(caption on next page)

Fig. 6. Establishment of prognostic risk model (A, B): The m6A-related prognostic lncRNA risk score model was established via Lasso regression. (C): The risk score distribution between the low-risk and high-risk groups of training group. (D): The survival status and survival time of patients in the two different risk groups of training group. (E): Risk-related heatmap of 4 m6A-related lncRNA in risk model. (F): Survival curve of the training group. (G): ROC curve of the training group to evaluate the accuracy of risk model.

4. Discussion

As a deathful brain tumor, glioblastoma multiforme has poor prognosis and can lead to death within six months without treatment [16]. Despite advances in its studies, GBM still poses a threat to patients by its characteristics such as its resistance to traditional therapies and its deep localization in the brain [16,17]. Although the incidence of GBM varies from 0.59 to 5 per 100,000 people in different countries, it is the highest in malignant primary brain tumors and has continually increased over the past decade [18,19]. m6A modification, the most abundant mRNA modification, was discovered in the 1970s during a study about methylation of mRNA in Novikoff hepatoma cells [20,21]. The reversibility of this modification is conferred by N6-methyltransferases and demethylases, which add and erase m6A methylation respectively [22]. In addition, modification of m6A on important mRNAs modulates mRNA metabolism, which consequently involves the regulation of cell fate [23]. In recent decades, emerging evidence suggests that m6A involves in cancer progression. Recent research reveals that compared with corresponding normal tissues, FTO in tumor tissues is remarkably increased, which promotes LUSC (lung squamous cell carcinoma) progression by its m6A demethylase role [24]. Another study indicates that in HSPCs (human hematopoietic stem/progenitor cells), the decrease of METTL3, a subunit of m6A methyltransferase, induces apoptosis and prevents leukemia progression [25,26]. Zhang S et al. demonstrated that by demethylating FOXM1 transcripts, m6A enzyme ALKBH5 increases FOXM1 expression, which enhances GSC (glioblastoma stem-like cells) tumorigenesis [27].

lncRNA is non-coding RNA transcripts composed of more than 200 nucleotides [28]. There are several studies demonstrating that m6A-related lncRNAs regulate the initiation and progression of multiple types of cancers. Recent research discovered that YTHDF1 and YTHDF2, which are m6A readers, function through reading m6A motifs and modulating the stability of lncRNA THOR in its m6A modification, thereby preserving the oncogenic capability of lncRNA THOR [29]. Yuan He et al. demonstrated that ALKBH5, a m6A eraser, is downregulated in pancreatic cancer cells, leading to demethylation of lncRNA KCN15-AS1 and regulation of cancer cell motility [30]. While in colorectal cancer, m6A methylation can promote the expression of lncRNA RP11, which further induces the dissemination of tumor cells [31].

Although there are numerous studies showing that m6A-related lncRNAs act as regulator in multiple cancers, the relationship between m6A-related lncRNAs and GBM remains unclear. Therefore, we constructed a prognostic model according to m6A-related lncRNAs which are expressed aberrantly in patients with GBM. These m6A-related lncRNAs also link to immune microenvironment.

Here, we obtained 13,251 lncRNAs and 23 m6A gene expression profiles from TCGA and GTEx (Genotype-Tissue Expression) dataset. These lncRNAs and m6A genes were then studied using Pearson correlation analysis, which helps us to determine 17 m6A-related lncRNAs. Next, based on Consensus clustering of m6A-related prognostic lncRNAs, patients were grouped into two clusters, which were cluster1 and cluster 2 respectively and both acted as subgroups of our prognostic model, with cluster 2 featuring worse survival probability and survival time than cluster 1.

Here, we determined by a consensus clustering approach how many subpopulations of GBM patients can be further divided in the best fit, based on the expression of prognostic correlated lncRNA. After this step of analysis, we determined that GBM patients could be divided into two different subsets to compare the analysis, and that the two subgroups were significantly different in prognosis, etc. Therefore, we accordingly divided the patients into high and low risk groups when we later established the prognostic evaluation model. Overall, the first step cluster analysis provides a direct reference for later modelled groups, with causal and supportive roles in logic. Also, the two clusters showed distinctive expression of CD274, with higher expression level in cluster 2, which may play a vital role in GBM. We further analyzed the different infiltration features of TME cells in these two clusters and evaluate 22 different immune cell types using CIBERSORT algorithm. Evidence indicates that there is an increase in the infiltration of immune cells of cluster 2 caused by its TME, which is also confirmed using ESTIMATE algorithm.

To explore the relationship between immune responses and m6A-related lncRNA, we first attempted to determine the link between immune cells and risk score. The results shows that infiltration fraction of several immune cells including T cells regulatory has positive correlation with risk score. Besides, we conducted enrichment analysis to study the immune response pathways related to m6A-related lncRNAs. The results of GSEA (Gene Set Enrichment Analysis) indicates that m6A-related lncRNAs involves in many immune response pathways including cytokine-cytokine receptor interaction, chemokine signaling pathway and tight junction. TGF β , which can be released by tumor cells and other cells in the TME, induces cancer progression through changing the architecture of tumors and inhibiting the anti-cancer activities of immune cells [32]. Research indicates that an elevated level of CCL18 is related to immunosuppressive nature of the TME, thus leading to a poor prognosis of patients [33]. Chu CW et al. found that thioridazine can promote P62-mediated autophagy and apoptosis in glioma cells by Wnt/ β -catenin signaling [34]. Consequently, the m6A-related lncRNAs involved in these biological process can be new targets for GBM therapy and prognosis evaluation.

In our research, a four -m6A-related lncRNAs risk model was constructed, which is composed of DLEU1, AC005005.3, ZEB1-AS1, UNC5B-AS1. Several studies have indicated that three of these lncRNAs are associated with cancer. Through recruiting SMARCA1, DLEU1 plays an essential role in KPNA3 activation, the high expression level of which suggests a poor prognosis of CRC (colorectal cancer) [35]. Ma MH et al. demonstrated that the ZEB1-AS1 can interact with miR-149-3p, constituting a miRNA-mediated ceRNA network to promote gastric cancer progression [36]. UNC5B-AS1 is supposed to act as an oncogene in thyroid cancer and its upregulation significantly link to lymph node metastasis and tumor size [37]. Although accumulating evidence shows that DLEU1,

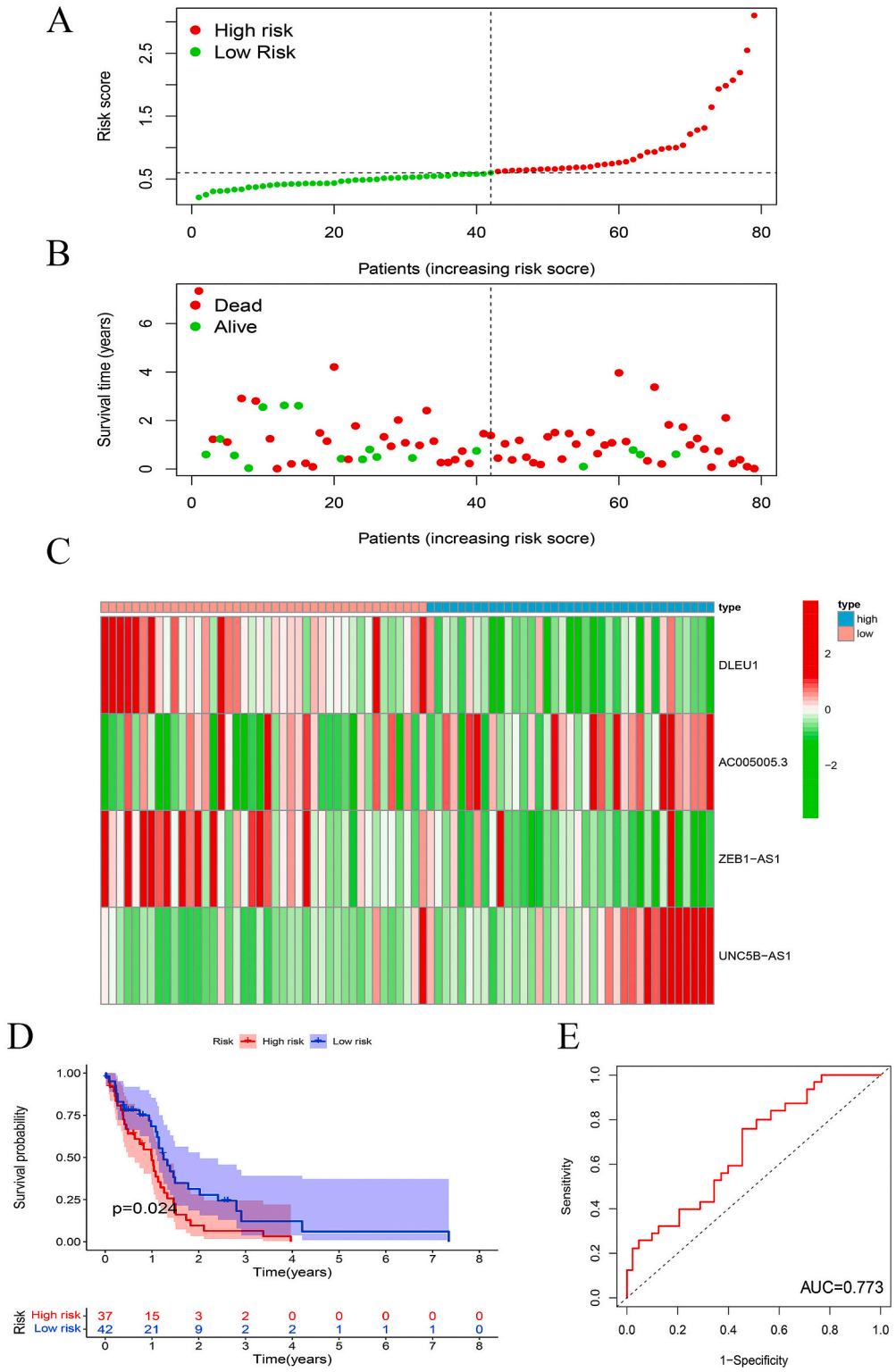
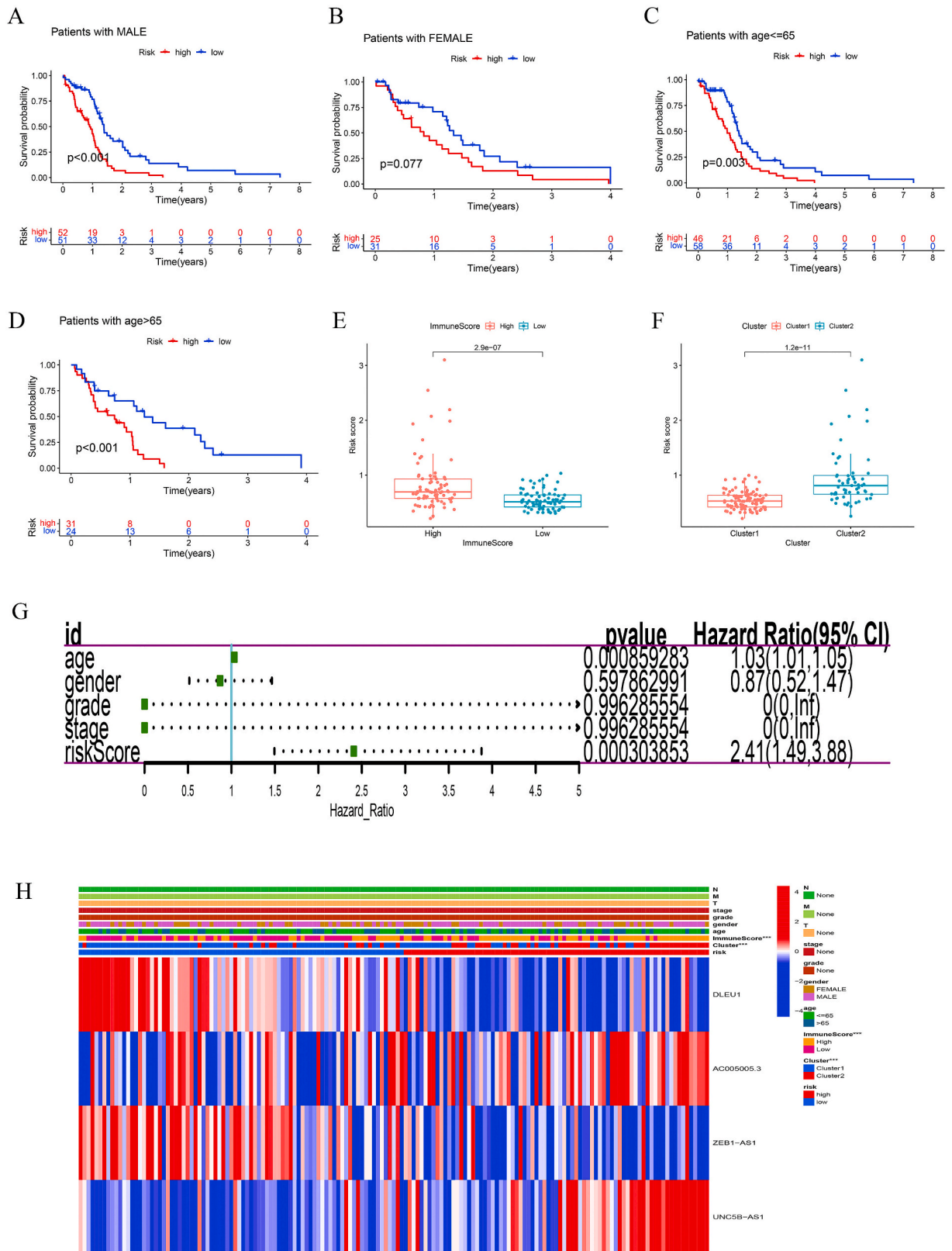


Fig. 7. Verification of risk model. (A): The risk score distribution between the low-risk and high-risk groups of test group. (B): The survival status and survival time of patients in the two different risk groups of test group. (C): Risk-related heatmap of 4 m6A-related lncRNA in risk model of test group. (D): Survival curve of the test group. (E): ROC curve of the test group to evaluate the accuracy of risk model.



(caption on next page)

Fig. 8. Correlation analysis to demonstrate relationship between prognostic risk model and clinical characteristics of GBM.

A–D: The Survival curve of patient with high or low risk in different clinical subgroups: age, gender. (E): Boxplot of correlation of risk score model and immune score. (F): Boxplot of correlation of risk score model and clusters. (G): Results of the COX regression analysis of whether risk score acts as an independent prognostic factor. (G): Heatmap of the differences in the expression of m6A-related prognostic lncRNAs between high-risk group and low-risk group.

ZEB1-AS1 and UNC5B-AS1 are associated with oncogenesis, there is little research of AC005005.3. Additionally, resources about the connection between other three lncRNA and GBM remain scarce. Our experiment suggests that DLEU1, AC005005.3, ZEB1-AS1 and UNC5B-AS1 may be associated with GBM prognosis and may be used as targets for GBM treatment. The accuracy of this four-m6A lncRNAs risk model was also verified by test set and there were significant prognostic differences between the high-risk and low-risk groups.

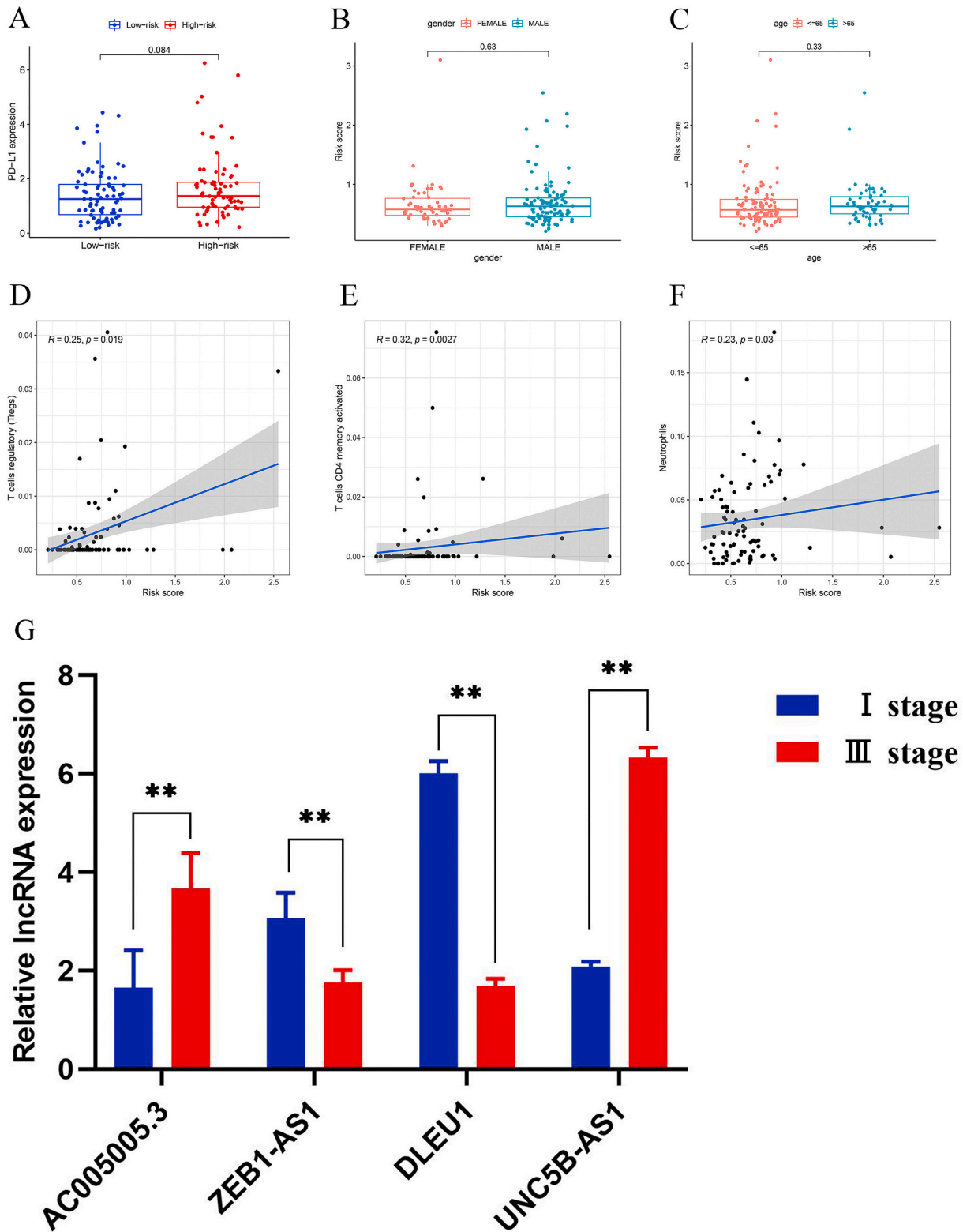
The tumor microenvironment (TME) is the environment surrounding a tumor, which includes the extracellular matrix, immune cells and blood vessels [38]. Numerous studies indicate that various immune cells including innate immune cells and adaptive immune cells induce cancer progression due to the influence of chemokines and cytokines secreted by tumor cells [39]. Thus, it is imperative to figure out the TME of GBM, which may provide valuable implications for immunotherapy. Our study suggests that m6A-related lncRNAs are related to immune response. Results show that the infiltration fractions of T cells regulatory (Treg), T cells CD8 and T cells CD4 memory activated are significantly correlated with worse clinical outcomes while the infiltration fraction of mast cells activated is related to better prognosis of patients with GBM. Accumulating evidence reveals that when plenty of Treg cells infiltrate into tumor, they can contribute to poor prognosis due to their suppression of anti-tumor immune response [40]. T cells CD8 are effectors in anticancer response but they may suffer dysfunction because of immunosuppression in the TME during tumor progression [41]. CD8 and CD4 T cells are key components of cancer immune cycle and take part in all steps. The failure of interaction of CD4 and CD8 in any step of this cycle can lead to unsuccessful tumor growth control [42]. Mast cells are capable to release various inflammatory mediators, which can induce or inhibit tumorigenesis [43]. Although many studies correlate immune cells with carcinogenesis, there are few experiments about the influence of m6A-related lncRNAs to infiltration fraction of immune cells in GBM. In our research, two clusters, which are grouped based on m6A-related lncRNA, show significant distinction in infiltration fraction of immune cells, immune score. Besides, our four-m6A-related lncRNA risk model links to immune response strongly. All the evidence suggests that these lncRNAs may be novel biomarkers for immune response of patients with GBM.

Compared with the previous similar glioma research related articles [44], our study included the sequence data from normal tissue samples in GTEx and was the first to construct a prognostic evaluation model for patients with GBM through m6a-related lncRNA. The study of Wang et al. [45] only used cox regression analysis to screen prognostic-related lncRNAs, and the study of Cai et al. [46] only used m6a regulators to classify patients into subtypes. Their study did not use machine learning methods to build a scoring model. We correlated m6a-related lncRNAs for analysis, established the corresponding risk assessment model and further subtyped patients. In addition, we also used clinical samples to experimentally verify the analysis results. And compared to the study of Xu et al. [47], our model is more efficient in evaluating the prognosis of patient (AUC = 0.795 vs 0.719).

Compared to the study of Tu et al. [48], we explored the immune cell subtypes associated with risk score, which were not done by their studies. Their study was limited to LGG patients rather than GBM patients, and there were not enough para-cancerous normal samples as controls in their study, which made the high-risk lncRNAs that they analyzed may be more common in para-cancerous normal tissues. High expression level. Our study included the sequencing data of normal tissue samples in GTEx, taking into account the difference between cancer tissues and normal tissues. Before starting the prognostic analysis, we first screened m6a-related lncRNAs and selected the differentially expressed lncRNAs. The lncRNAs we screened are all differentially expressed in adjacent and cancerous tissues, and were related to m6a and patient prognosis, which was not achieved in the study of Tu et al.

4 lncRNA were selected to be closely related to the prognosis of patients, establishing the four-m6A-related lncRNAs prognostic model. According to this model, the samples in training set were divided into high-risk and low-risk groups based on median risk score, with high-risk group showing poor prognostic features. The prognostic value of this risk model is also demonstrated by the test set and receiver operating characteristic (ROC) curve showed the better performance of this model in predicting GBM OS than conventional clinical characteristics. Furthermore, according to general clinicopathological characteristics covering gender and age, stratified analysis was conducted to verify that the high-risk group had a poorer prognosis compared with low-risk group. As an independent predictor for GBM OS, m6A-related lncRNA risk model is strongly related to immune score and clusters, and can perform an accurate prognosis for patients. Therefore, our research illustrated the interplay between m6A and lncRNA, and offered a novel prospect of prognostic markers of GBM, which may bring hope for patients suffering from GBM.

Nevertheless, there are also certain limitations in our study. These four m6A-related lncRNA need to be validated using more clinical samples and the risk model also need to be improved by more clinical data. In terms of model construction, this study used lasso regression analysis and cox regression analysis rather than random forest methods, which makes the model's prediction efficiency may not be the highest. Compared to lasso regression analysis, random forest algorithm modeling has the following advantages: during the training process, random forest algorithm is able to detect the interactions between FEATURES and does not have to do feature selection (because the feature subset is randomly selected); when creating random forest, unbiased estimation is used for generalization error, and the model generalization ability is strong; In addition, it can balance the error for unbalanced datasets and maintain accuracy even if a large portion of features are missing. Also, more biological experiments are required to be conducted to understand the molecular mechanisms by which those m6A-related lncRNA affects the prognosis.



(caption on next page)

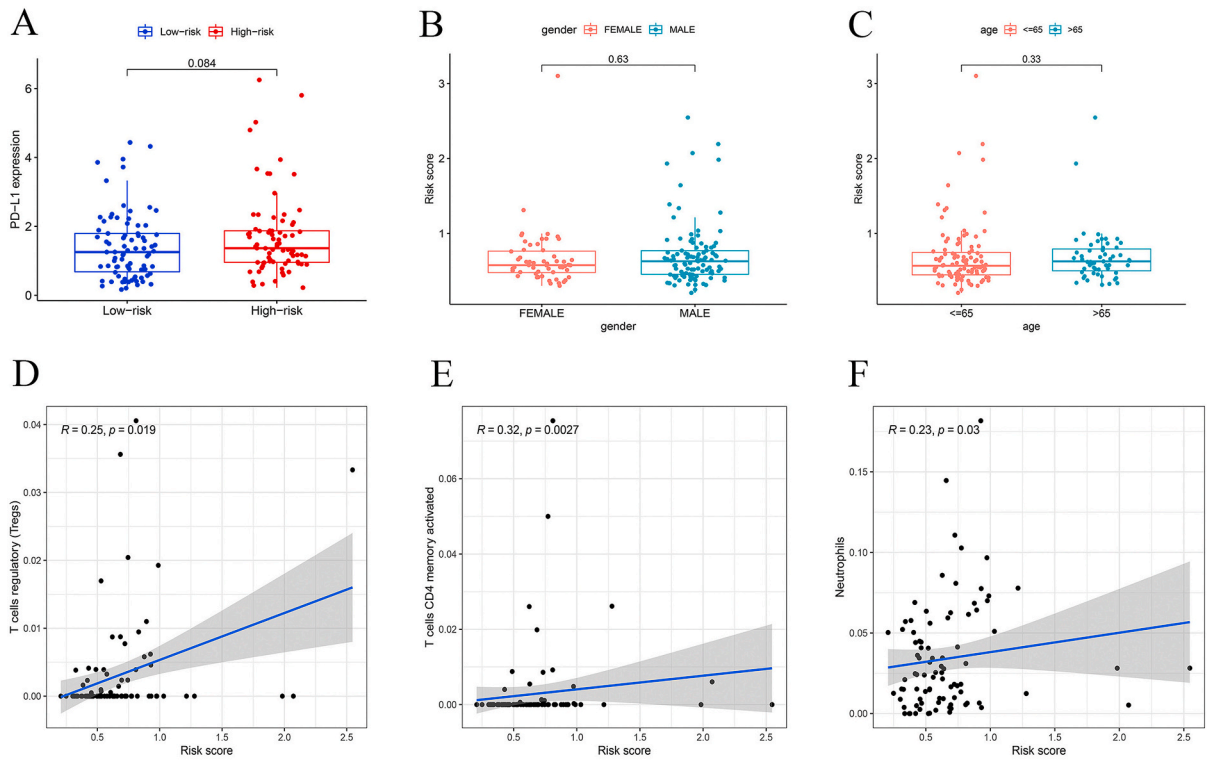


Fig. 9. Correlation between immune-infiltrating cells, clinical character and risk score in GBM (A): Differences in the expression of *PD-L1* in high-risk group and low-risk group. (B): Differences of risk score in the male and female group. (C): Differences of risk score in the different ages group. (D–F): Scatterplot of correlation analysis of risk score and immune-infiltrating cells. T cells regulatory (Tregs) T cells CD4 memory activated and neutrophils were positive correlated with the risk scores, $P < 0.05$. (G):qPCR results of the expression of prognostic related model lncRNA. ** represents a p-value less than 0.01.

5. Conclusion

To summarize, we constructed a four m6A-related lncRNAs risk model, which can predict the prognosis of patients with GBM, thus providing new insights into the treatment of GBM patients. Additionally, our research also found a significant relationship between m6A-related prognostic lncRNAs and immune response pathways, indicating the potential of finding biomarkers for immunotherapies in patients of this cancer.

Data availability statement

Data will be made available on request.

Author contributions

Qisheng Luo:Conceived and designed the experiments; Analyzed and interpreted the data; Wrote the paper. Zhenxiu Yang: Performed the experiments; Contributed reagents, materials, analysis tools or data; Wrote the paper. Renzhi Deng:Performed the experiments; Wrote the paper. Xianhui Pang:Performed the experiments; Wrote the paper. Xu Han:Performed the experiments; Analyzed and interpreted the data; Xinfu Liu:Performed the experiments; Contributed reagents, materials, analysis tools or data; Jiahai Du: Analyzed and interpreted the data; Contributed reagents, materials, analysis tools or data; Yingzhao Tian: Performed the experiments; Contributed reagents, materials, analysis tools or data; Jingzhan Wu: Conceived and designed the experiments; Contributed reagents, materials, analysis tools or data; Chunhai Tang: Conceived and designed the experiments; Contributed reagents, materials, analysis tools or data; Wrote the paper.

Ethics approval and consent to participate

The data used for the construction of model in this work were acquired from the publicly available datasets. This study was conducted in accordance with the recommendations of the Ethics Committee of the Second Affiliated Hospital of Guangxi Medical University. The protocol was approved by the Ethics Committee of the Second Affiliated Hospital of Guangxi Medical University. All subjects gave written informed consent in accordance with the Declaration of Helsinki.

Funding

1. National Natural Science Foundation of China, Grant/Award Number: 81760450; 2. Guangxi Natural Science Foundation of China, Grant/Award Number: 2019GXNSFDA245034; 3. The First Batch of High-level Talent Scientific Research Projects of the Affiliated Hospital of Youjiang Medical University for Nationalities in 2019 (Contract No. R20196310); 4. The Self-funded project of Guangxi Health Commission (Contract No. Z20210933,Z-A20220582); 5. The self-funded project of Guangxi Autonomous Region Administration of Traditional Chinese Medicine (Contract No. ZXZYA20220242); 6. Supported by the R&D project of Guangxi Zhuang Autonomous Region Key Trauma Surgery (Contract No. GKTS2022).

Declaration of competing interest

The authors declare that no conflict of interest exists.

References

- [1] Glioblastoma Multiforme – Symptoms, Diagnosis and Treatment Options (aans.org).
- [2] Survival Rates for Selected Adult Brain and Spinal Cord Tumors (cancer.org).
- [3] Glioblastoma Prognosis, Brain Tumour Survival Rates (thebraintumourcharity.org).
- [4] L. He, H. Li, A. Wu, Y. Peng, G. Shu, G. Yin, Functions of N6-methyladenosine and its role in cancer, *Mol. Cancer* 18 (1) (2019 Dec 4) 176, <https://doi.org/10.1186/s12943-019-1109-9>. PMID: 31801551; PMCID: PMC6892141.
- [5] Y. Yang, P.J. Hsu, Y.S. Chen, Y.G. Yang, Dynamic transcriptomic m6A decoration: writers, erasers, readers and functions in RNA metabolism, *Cell Res.* 28 (6) (2018 Jun) 616–624, <https://doi.org/10.1038/s41422-018-0040-8>. Epub 2018 May 22. PMID: 29789545; PMCID: PMC5993786.
- [6] D. Dai, H. Wang, L. Zhu, H. Jin, X. Wang, N6-methyladenosine links RNA metabolism to cancer progression, *Cell Death Dis.* 9 (2) (2018 Jan 26) 124, <https://doi.org/10.1038/s41419-017-0129-x>. PMID: 29374143; PMCID: PMC5833385.
- [7] T. Sun, R. Wu, L. Ming, The role of m6A RNA methylation in cancer, *Biomed. Pharmacother.* 112 (2019 Apr), 108613, <https://doi.org/10.1016/j.biopha.2019.108613>. Epub 2019 Feb 19. PMID: 30784918.
- [8] L. He, H. Li, A. Wu, Y. Peng, G. Shu, G. Yin, Functions of N6-methyladenosine and its role in cancer, *Mol. Cancer* 18 (1) (2019 Dec 4) 176, <https://doi.org/10.1186/s12943-019-1109-9>. PMID: 31801551; PMCID: PMC6892141.

- [9] M. Chen, L. Wei, C.T. Law, F.H. Tsang, J. Shen, C.L. Cheng, L.H. Tsang, D.W. Ho, D.K. Chiu, J.M. Lee, C.C. Wong, I.O. Ng, C.M. Wong, RNA N6-methyladenosine methyltransferase-like 3 promotes liver cancer progression through YTHDF2-dependent posttranscriptional silencing of SOCS2, *Hepatology* 67 (6) (2018 Jun) 2254–2270, <https://doi.org/10.1002/hep.29683>. Epub 2018 Apr 19. PMID: 29171881.
- [10] J. Li, S. Meng, M. Xu, S. Wang, L. He, X. Xu, X. Wang, L. Xie, Downregulation of N6-methyladenosine binding YTHDF2 protein mediated by miR-493-3p suppresses prostate cancer by elevating N6-methyladenosine levels, *Oncotarget* 9 (3) (2017 Dec 18) 3752–3764, <https://doi.org/10.18632/oncotarget.23365>. PMID: 29423080; PMCID: PMC5790497.
- [11] Q. Cui, H. Shi, P. Ye, L. Li, Q. Qu, G. Sun, G. Sun, Z. Lu, Y. Huang, C.G. Yang, A.D. Riggs, C. He, Y. Shi, m6A RNA methylation regulates the self-renewal and tumorigenesis of glioblastoma stem cells, *Cell Rep.* 18 (11) (2017 Mar 14) 2622–2634, <https://doi.org/10.1016/j.celrep.2017.02.059>. PMID: 28297667; PMCID: PMC5479356.
- [12] G. Yang, X. Lu, L. Yuan, lncRNA: a link between RNA and cancer, *Biochim. Biophys. Acta* 1839 (11) (2014 Nov) 1097–1109, <https://doi.org/10.1016/j.bbagr.2014.08.012>. Epub 2014 Aug 23. PMID: 25159663.
- [13] Q. Li, C. Dong, J. Cui, Y. Wang, X. Hong, Over-expressed lncRNA HOTAIRM1 promotes tumor growth and invasion through up-regulating HOXA1 and sequestering G9a/EZH2/Dnmts away from the HOXA1 gene in glioblastoma multiforme, *J. Exp. Clin. Cancer Res.* 37 (1) (2018 Oct 30) 265, <https://doi.org/10.1186/s13046-018-0941-x>. PMID: 30376874; PMCID: PMC6208043.
- [14] Z. Li, J. Zhang, H. Zheng, C. Li, J. Xiong, W. Wang, H. Bao, H. Jin, P. Liang, Modulating lncRNA SNHG15/CDK6/miR-627 circuit by palbociclib, overcomes temozolomide resistance and reduces M2-polarization of glioma associated microglia in glioblastoma multiforme, *J. Exp. Clin. Cancer Res.* 38 (1) (2019 Aug 28) 380, <https://doi.org/10.1186/s13046-019-1371-0>. PMID: 31462285; PMCID: PMC6714301.
- [15] S. Wang, F. Yao, X. Lu, Q. Li, Z. Su, J.H. Lee, C. Wang, L. Du, Temozolomide promotes immune escape of GBM cells via upregulating PD-L1, *Am J Cancer Res* 9 (6) (2019 Jun 1) 1161–1171. PMID: 31285949; PMCID: PMC6610056.
- [16] Glioblastoma Multiforme – Symptoms, Diagnosis and Treatment Options (aans.org).
- [17] Glioblastoma - Overview - Mayo Clinic.
- [18] A.F. Tamimi, M. Juweid, Epidemiology and outcome of glioblastoma, in: S. De Vleeschouwer (Ed.), *Glioblastoma*, Codon Publications, Brisbane (AU), 2017 Sep 27 (Chapter 8). PMID: 29251870.
- [19] N. Grech, T. Dalli, S. Mizzi, L. Meilak, N. Calleja, A. Zrinzo, Rising incidence of glioblastoma multiforme in a well-defined population, *Cureus* 12 (5) (2020 May 19), e8195, <https://doi.org/10.7759/cureus.8195>. PMID: 32572354; PMCID: PMC7302718.
- [20] Y. Yang, P.J. Hsu, Y.S. Chen, Y.G. Yang, Dynamic transcriptomic m6A decoration: writers, erasers, readers and functions in RNA metabolism, *Cell Res.* 28 (6) (2018 Jun) 616–624, <https://doi.org/10.1038/s41422-018-0040-8>. Epub 2018 May 22. PMID: 29789545; PMCID: PMC5993786.
- [21] R. Desrosiers, K. Friderici, F. Rottman, Identification of methylated nucleosides in messenger RNA from Novikoff hepatoma cells, *Proc. Natl. Acad. Sci. U. S. A.* 71 (10) (1974 Oct) 3971–3975, <https://doi.org/10.1073/pnas.71.10.3971>. PMID: 4372599; PMCID: PMC434308.
- [22] Y. Fu, D. Dominissini, G. Rechavi, C. He, Gene expression regulation mediated through reversible m⁶A RNA methylation, *Nat. Rev. Genet.* 15 (5) (2014 May) 293–306, <https://doi.org/10.1038/nrg3724>. Epub 2014 Mar 25. PMID: 24662220.
- [23] H. Gan, L. Hong, F. Yang, D. Liu, L. Jin, Q. Zheng, Progress in epigenetic modification of mRNA and the function of m6A modification, *Sheng Wu Gong Cheng Xue Bao* 35 (5) (2019 May 25) 775–783, <https://doi.org/10.13345/j.cjb.180416>. PMID: 31222996.
- [24] J. Liu, D. Ren, Z. Du, H. Wang, H. Zhang, Y. Jin, m6A demethylase FTO facilitates tumor progression in lung squamous cell carcinoma by regulating MZF1 expression, *Biochem. Biophys. Res. Commun.* 502 (4) (2018 Aug 25) 456–464, <https://doi.org/10.1016/j.bbrc.2018.05.175>. Epub 2018 Jun 2. PMID: 29842885.
- [25] L.P. Vu, B.F. Pickering, Y. Cheng, S. Zaccara, D. Nguyen, G. Minuesa, T. Chou, A. Chow, Y. Saletore, M. MacKay, J. Schulman, C. Famulare, M. Patel, V. M. Klimek, F.E. Garrett-Bakelman, A. Melnick, M. Carroll, C.E. Mason, S.R. Jaffrey, M.G. Kharas, The N6-methyladenosine (m6A)-forming enzyme METTL3 controls myeloid differentiation of normal hematopoietic and leukemia cells, *Nat. Med.* 23 (11) (2017 Nov) 1369–1376, <https://doi.org/10.1038/nm.4416>. Epub 2017 Sep 18. PMID: 28920958; PMCID: PMC5677536.
- [26] <https://www.ncbi.nlm.nih.gov/gene?Db=gene&Cmd=ShowDetailView&TermToSearch=56339>.
- [27] S. Zhang, B.S. Zhao, A. Zhou, K. Lin, S. Zheng, Z. Lu, Y. Chen, E.P. Sulman, K. Xie, O. Bögl, S. Majumder, C. He, S. Huang, m6A demethylase ALKBH5 maintains tumorigenicity of glioblastoma stem-like cells by sustaining FOXM1 expression and cell proliferation program, *e6*, *Cancer Cell* 31 (4) (2017 Apr 10) 591–606, <https://doi.org/10.1016/j.ccell.2017.02.013>. Epub 2017 Mar 23. PMID: 28344040; PMCID: PMC5427719.
- [28] W.X. Peng, P. Koirala, Y.Y. Mo, lncRNA-mediated regulation of cell signaling in cancer, *Oncogene* 36 (41) (2017 Oct 12) 5661–5667, <https://doi.org/10.1038/nc.2017.184>. Epub 2017 Jun 12. PMID: 28604750; PMCID: PMC6450570.
- [29] H. Liu, Y. Xu, B. Yao, T. Sui, L. Lai, Z. Li, A novel N6-methyladenosine (m6A)-dependent fate decision for the lncRNA THOR, *Cell Death Dis.* 11 (8) (2020 Aug 13) 613, <https://doi.org/10.1038/s41419-020-02833-y>. PMID: 32792482; PMCID: PMC7426843.
- [30] Y. He, H. Hu, Y. Wang, H. Yuan, Z. Lu, P. Wu, D. Liu, L. Tian, J. Yin, K. Jiang, Y. Miao, ALKBH5 inhibits pancreatic cancer motility by decreasing long non-coding RNA KCNK15-AS1 methylation, *Cell. Physiol. Biochem.* 48 (2) (2018) 838–846, <https://doi.org/10.1159/000491915>. Epub 2018 Jul 20. Erratum in: *Cell Physiol Biochem.* 2019;52(5):1254. PMID: 30032148.
- [31] Y. Wu, X. Yang, Z. Chen, L. Tian, G. Jiang, F. Chen, J. Li, P. An, L. Lu, N. Luo, J. Du, H. Shan, H. Liu, H. Wang, m6A-induced lncRNA RP11 triggers the dissemination of colorectal cancer cells via upregulation of Zeb1, *Mol. Cancer* 18 (1) (2019 Apr 13) 87, <https://doi.org/10.1186/s12943-019-1014-2>. PMID: 30979372; PMCID: PMC6461827.
- [32] R. Derynck, S.J. Turley, R.J. Akhurst, TGF β biology in cancer progression and immunotherapy, *Nat. Rev. Clin. Oncol.* 18 (1) (2021 Jan) 9–34, <https://doi.org/10.1038/s41571-020-0403-1>. Epub 2020 Jul 24. PMID: 32710082.
- [33] J. Korbecki, M. Olbromski, P. Dziegiel, CCL18 in the progression of cancer, *Int. J. Mol. Sci.* 21 (21) (2020 Oct 26) 7955, <https://doi.org/10.3390/ijms21217955>. PMID: 33114763; PMCID: PMC7663205.
- [34] C.W. Chu, H.J. Ko, C.H. Chou, T.S. Cheng, H.W. Cheng, Y.H. Liang, Y.L. Lai, C.Y. Lin, C. Wang, J.K. Loh, J.T. Cheng, S.J. Chiou, C.L. Su, C.F. Huang, Y.R. Hong, Thioridazine enhances P62-mediated autophagy and apoptosis through wnt/ β -catenin signaling pathway in glioma cells, *Int. J. Mol. Sci.* 20 (3) (2019 Jan 22) 473, <https://doi.org/10.3390/ijms20030473>. PMID: 30678307; PMCID: PMC6386927.
- [35] T. Liu, Z. Han, H. Li, Y. Zhu, Z. Sun, A. Zhu, lncRNA DLEU1 contributes to colorectal cancer progression via activation of KPNA3, *Mol. Cancer* 17 (1) (2018 Aug 11) 118, <https://doi.org/10.1186/s12943-018-0873-2>. PMID: 30098595; PMCID: PMC6087004.
- [36] M.H. Ma, J.X. An, C. Zhang, J. Liu, Y. Liang, C.D. Zhang, Z. Zhang, D.Q. Dai, ZEB1-AS1 initiates a miRNA-mediated ceRNA network to facilitate gastric cancer progression, *Cancer Cell Int.* 19 (2019 Feb 6) 27, <https://doi.org/10.1186/s12935-019-0742-0>. Erratum in: *Cancer Cell Int.* 2019 Apr 11;19:95. PMID: 30774556; PMCID: PMC6364449.
- [37] Y. Wang, A. Bhandari, J. Niu, F. Yang, E. Xia, Z. Yao, Y. Jin, Z. Zheng, S. Lv, O. Wang, The lncRNA UNC5B-AS1 promotes proliferation, migration, and invasion in papillary thyroid cancer cell lines, *Hum. Cell* 32 (3) (2019 Jul) 334–342, <https://doi.org/10.1007/s13577-019-00242-8>. Epub 2019 Feb 25. PMID: 30805847.
- [38] What is the tumor microenvironment? MD Anderson Cancer Center.
- [39] D.C. Hinshaw, L.A. Shevde, The tumor microenvironment innately modulates cancer progression, *Cancer Res.* 79 (18) (2019 Sep 15) 4557–4566, <https://doi.org/10.1158/0008-5472.CAN-18-3962>. Epub 2019 Jul 26. PMID: 31350295; PMCID: PMC6744958.
- [40] A. Tanaka, S. Sakaguchi, Regulatory T cells in cancer immunotherapy, *Cell Res.* 27 (1) (2017 Jan) 109–118, <https://doi.org/10.1038/cr.2016.151>. Epub 2016 Dec 20. PMID: 27995907; PMCID: PMC5223231.
- [41] B. Farhood, M. Najafi, K. Mortezaee, CD8+ cytotoxic T lymphocytes in cancer immunotherapy: a review, *J. Cell. Physiol.* 234 (6) (2019 Jun) 8509–8521, <https://doi.org/10.1002/jcp.27782>. Epub 2018 Nov 22. PMID: 30520029.
- [42] D. Ostromov, N. Fekete-Drimusz, M. Saborowski, F. Kühnel, N. Woller, CD4 and CD8 T lymphocyte interplay in controlling tumor growth, *Cell. Mol. Life Sci.* 75 (4) (2018 Feb) 689–713, <https://doi.org/10.1007/s00118-017-2686-7>. Epub 2017 Oct 14. PMID: 29032503; PMCID: PMC5769828.
- [43] Y. Gorzalczany, R. Sagi-Eisenberg, Role of mast cell-derived adenosine in cancer, *Int. J. Mol. Sci.* 20 (10) (2019 May 27) 2603, <https://doi.org/10.3390/ijms20102603>. PMID: 31137883; PMCID: PMC6566897.

- [44] S. Lin, H. Xu, A. Zhang, Y. Ni, Y. Xu, T. Meng, M. Wang, M. Lou, Prognosis analysis and validation of m6A signature and tumor immune microenvironment in glioma, *Front. Oncol.* 10 (2020 Oct 5), 541401, <https://doi.org/10.3389/fonc.2020.541401>.
- [45] W. Wang, J. Li, F. Lin, J. Guo, J. Zhao, Identification of N6-methyladenosine-related lncRNAs for patients with primary glioblastoma, *Neurosurg. Rev.* 44 (1) (2021 Feb) 463–470.
- [46] Z. Cai, J. Zhang, Z. Liu, J. Su, J. Xu, Z. Li, H. Meng, H. Zhang, M. Huang, D. Zhao, C. Duan, X. He, Identification of an N6-methyladenosine (m6A)-related signature associated with clinical prognosis, immune response, and chemotherapy in primary glioblastomas, *Ann. Transl. Med.* 9 (15) (2021 Aug) 1241, <https://doi.org/10.21037/atm-21-3139>.
- [47] S. Xu, L. Tang, G. Dai, C. Luo, Z. Liu, Expression of m6A regulators correlated with immune microenvironment predicts therapeutic efficacy and prognosis in gliomas, *Front. Cell Dev. Biol.* 8 (2020 Nov 10), 594112, <https://doi.org/10.3389/fcell.2020.594112>.
- [48] Z. Tu, L. Wu, P. Wang, Q. Hu, C. Tao, K. Li, K. Huang, X. Zhu, N6-Methyladenosine-Related lncRNAs are potential biomarkers for predicting the overall survival of lower-grade glioma patients, *Front. Cell Dev. Biol.* 8 (2020 Jul 23) 642, <https://doi.org/10.3389/fcell.2020.00642>.